Fermilab

Comparing the DES-SN5YR and Pantheon+ SN cosmology analyses: Investigation based on "Evolving Dark Energy or Supernovae systematics?"

FERMILAB-PUB-24-0950-PPD

arXiv:2501.06664

MNRAS 000, 1–9 (2025) Preprint 14 January 2025 Compiled using MNRAS LATEX style file v3.3
FERMILAB-PUB-24-0950-PPD

Comparing the DES-SN5YR and Pantheon+ SN cosmology analyses: Investigation based on "Evolving Dark Energy or Supernovae systematics?"

M. Vincenzi,[1★] R. Kessler,[2,3] P. Shah,[4] J. Lee,[5] T. M. Davis,[6] D. Scolnic,[7] P. Armstrong,[12] D. Brout,[8] R. Camilleri,[6] R. Chen,[7] L. Galbany,[9,10] C. Lidman,[11,12] A. Möller,[13] B. Popovic,[14] B. Rose,[15] M. Sako,[5] B. O. Sánchez,[16] M. Smith,[17] M. Sullivan,[18] P. Wiseman,[18] T. M. C. Abbott,[19] M. Aguena,[20] S. Allam,[21] F. Andrade-Oliveira,[22] S. Bocquet,[23] D. Brooks,[4] A. Carnero Rosell,[24,20,25] J. Carretero,[26] L. N. da Costa,[20] M. E. S. Pereira,[27] H. T. Diehl,[21] P. Doel,[4] S. Everett,[28] B. Flaugher,[21] J. Frieman,[21,3] J. García-Bellido,[29] E. Gaztanaga,[10,30,9] D. Gruen,[23] R. A. Gruendl,[31,32] G. Gutierrez,[21] S. R. Hinton,[6] D. L. Hollowood,[33] K. Honscheid,[34,35] D. J. James,[36] K. Kuehn,[37,38] O. Lahav,[4] S. Lee,[39] J. L. Marshall,[40] J. Mena-Fernández,[41] R. Miquel,[42,26] J. Muir,[43] J. Myles,[44] A. Palmese,[45] A. A. Plazas Malagón,[46,47] A. Porredon,[48,49] S. Samuroff,[50,26] E. Sanchez,[48] D. Sanchez Cid,[48] I. Sevilla-Noarbe,[48] E. Suchyta,[51] G. Tarle,[52] C. To,[34] D. L. Tucker,[21] V. Vikram,[22] A. R. Walker,[19] N. Weaverdyck,[53,54] and J. Weller[55,56]

(DES Collaboration)

Accepted XXX. Received YYY; in original form ZZZ

ABSTRACT

Recent cosmological analyses measuring distances of Type Ia Supernovae (SNe Ia) and Baryon Acoustic Oscillations (BAO) have all given similar hints at time-evolving dark energy. To examine whether underestimated SN Ia systematics might be driving these results, Efstathiou (2024) compared overlapping SN events between Pantheon+ and DES-SN5YR (20% SNe are in common), and reported evidence for a ∼0.04 mag offset between the low and high-redshift distance measurements of this subsample of events. If these offsets are arbitrarily subtracted from the entire DES-SN5YR sample, the preference for evolving dark energy is reduced. In this paper, we reproduce this offset and show that it has two sources. First, 43% of the offset is due to DES-SN5YR improvements in the modelling of supernova intrinsic scatter and host galaxy properties. These are scientifically-motivated modelling updates implemented in DES-SN5YR and their associated uncertainties are captured within the DES-SN5YR systematic error budget. Even if the less accurate scatter model and host properties from Pantheon+ are used instead, the DES-SN5YR evidence for evolving dark energy is only reduced from 3.9σ to 3.3σ. Second, 38% of the offset is due to a misleading comparison because different selection functions characterize the DES subsets included in Pantheon+ and DES-SN5YR and therefore individual SN distance measurements are *expected* to be different because of different bias corrections. In conclusion, we confirm the validity of the published DES-SN5YR results.

Key words: supernovae, cosmology, dark energy

1 CONTEXT

The cosmological results from the Dark Energy Survey Supernova Program (DES-SN) have been published in two stages: (1) a small *spectroscopically classified* subset of ∼ 200 events combined with ∼100 previously released low-z events from the community (DES-SN3YR: Brout et al. 2019b; Abbott et al. 2019), and (2) a more complete *photometrically classified* sample of 1600 events, combined with ∼190 low-z events from the community (DES-SN5YR: Vincenzi et al. 2024; DES Collaboration et al. 2024). In between these two efforts, a much larger *spectroscopically confirmed* sample of 1,701 publicly released light-curves was used to publish cosmology constraints (Pantheon+: Brout et al. 2022a; Scolnic et al. 2022). While Pantheon+ is technically not a DES-SN result, the Pantheon+ and DES-SN5YR analyses included a significant overlap of software (Kessler et al. 2009; Hinton & Brout 2020; Zuntz et al. 2015), people and development, particularly for the intrinsic scatter modelling based on dust (Brout & Scolnic 2021; Popovic et al. 2023) and Beams with Bias Corrections (BBC: Kessler & Scolnic 2017).

At low redshifts ($z < 0.1$), there is significant sample overlap

★ E-mail: maria.vincenzi@physics.ox.ac.uk

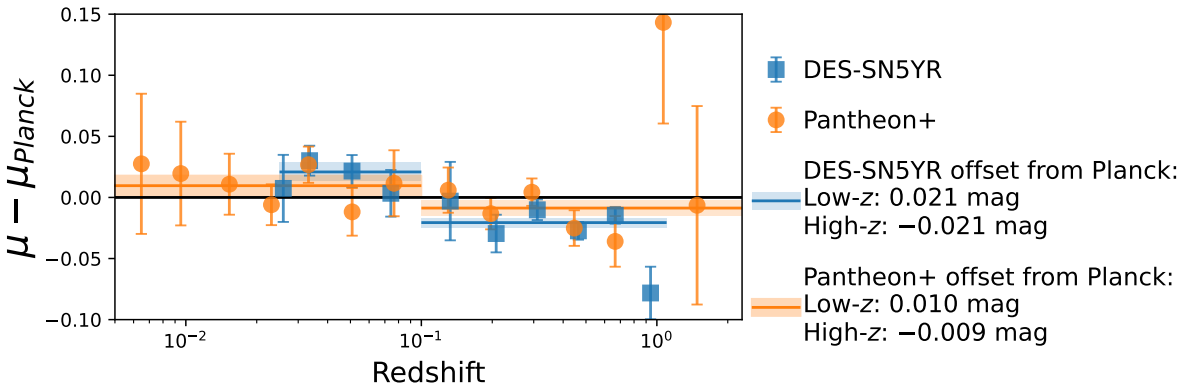

Figure 1. Pantheon+ and DES-SN5YR binned Hubble residuals calculated w.r.t. a FlatΛCDM cosmology assuming $\Omega_M = 0.315$ from *Planck*. In each redshift bin we show the weighted mean of the Hubble residual and statistical-only uncertainties. The horizontal bands show the weighted mean of the Hubble residuals (and associated uncertainties) above and below redshift 0.1 for both Pantheon+ and DES-SN5YR.

between Pantheon+ and DES-SN5YR. More than 90% of the low-z SNe in DES-SN5YR are also included in Pantheon+ (184 low-z overlapping events in total, 118 from the Foundation SN sample, 59 from CfA SN programs and 7 from the Carnegie Supernova Project; Hicken et al. 2009, 2012; Krisciunas et al. 2017; Foley et al. 2017). Pantheon+ includes ∼ 500 additional low-z events that were not included in DES-SN5YR to minimize low-z related systematics (in particular, calibration uncertainties). At high redshifts ($z > 0.1$), sample overlap between Pantheon+ and DES-SN5YR includes 145 common DES SN events, which is ∼8% of the DES-SN5YR high-z sample and ∼14% of the Pantheon+ high-z sample.

The binned Pantheon+ and DES-SN5YR Hubble diagram residuals are compared in Fig. 1 with respect to (w.r.t.) a FlatΛCDM cosmology model assuming the *Planck* best-fit dark matter energy density $\Omega_M = 0.315$ (Planck Collaboration et al. 2020b). The binned Hubble residuals are consistent within 1σ in every bin between Pantheon+ and DES-SN5YR, and both datasets show a discrepancy w.r.t. *Planck*. Discrepancies are in the same direction (positive residuals at low-z and negative residuals at high-z) but for DES-SN5YR the effect is larger (± ∼ 0.02 mag discrepancies for DES-SN5YR compared to ± ∼0.01 mag discrepancies for Pantheon+) and uncertainties are smaller due to improved light curve modelling and larger high-z statistics. Using flat priors on cosmology parameters the "SN-only" Pantheon+ and DES-SN5YR analyses found consistent results in FlatΛCDM ($\Omega_M = 0.334 \pm 0.018$ and $\Omega_M = 0.352 \pm 0.017$ respectively) and Flat$w$CDM ($w = -0.90 \pm 0.14$ and $w = -0.80^{+0.14}_{-0.16}$ respectively, see also Fig. 12 in DES Collaboration et al. 2024). In Flatw_0w_aCDM,[1] the results are consistent to $\sim 2\sigma$,

Pantheon+: $w_0 = -0.93 \pm 0.15$, $w_a = -0.1^{+0.9}_{-2.0}$,
DES SN5YR: $w_0 = -0.36^{+0.36}_{-0.30}$, $w_a = -8.8^{+3.7}_{-4.5}$.

While the Pantheon+ distance uncertainties are larger compared to DES-SN5YR, the Pantheon+ cosmology uncertainties are smaller because of the (i) larger redshift range (0.001 to 2.26) compared to the DES-SN5YR redshift range (0.025 to 1.13), and (ii) additional systematic uncertainties included in DES-SN5YR.

Shortly after the DES-SN5YR constraints were published, the Dark Energy Spectroscopic Instrument (DESI) Collaboration released cosmological results from the measurement of BAO in galaxy, quasar and Lyman-α forest tracers from the first year of observations (DESI-BAO-Y1, DESI Collaboration et al. 2024). When combining DESI with CMB measurements (CMB anisotropies from *Planck* and CMB lensing data from *Planck* and ACT, Carron et al. 2022; Planck Collaboration et al. 2020a), a 2.6σ evidence for time-varying dark energy equation of state is found. This evidence is unchanged when the Pantheon+ SN constraints are added (2.5σ evidence), but grows to 3.9σ when DES-SN5YR constraints are used instead of Pantheon+. These tantalizing hints for dynamical dark energy have motivated further scrutiny of these cosmological results, and re-analyses have focused on public data releases from Pantheon+ and DES-SN5YR.

Other than DES-SN and Pantheon+, there was a another cosmological analysis using more than 2,000 spectroscopically confirmed SNe Ia from public data releases: the UNION3 compilation (Rubin et al. 2023). For the FlatΛCDM model, they found results consistent with DES-SN5YR and Pantheon+ (best-fit $\Omega_M = 0.356^{+0.028}_{-0.026}$). For the Flat$w$CDM model, they found $w = -0.74^{+0.17}_{-0.19}$, a slightly larger deviation from a cosmological constant compared to DES-SN5YR and Pantheon+. They do not publish SN-only results for the Flatw_0w_aCDM model. When UNION3 is combined with DESI BAO and CMB, there is a 3.1σ evidence for time-evolving dark energy. The UNION3 sample has a large overlap of supernova light-curves with Pantheon+. However, the UNION3 analysis used a Bayesian hierarchical framework 'Unity' (Rubin et al. 2015), which is very different from the methodology used in Pantheon+ and DES-SN5YR. UNION3 has not released a Hubble diagram, and therefore we do not include UNION3 comparisons in this investigation.

2 RECENT ANALYSIS BY EFSTATHIOU (2024)

Efstathiou (2024) examined publicly released Hubble diagrams from Pantheon+ and DES-SN5YR, and performed a distance comparison with the overlapping SNe that are used in both samples. Efstathiou (2024) notes a ∼0.04 mag discrepancy in standardized brightnesses between the low-z and high-z overlapping events in Pantheon+ and DES-SN5YR. He suggests that this discrepancy is the reason why the DES-SN5YR sample provides more significant evidence for evolving dark energy compared to Pantheon+ and, in FlatΛCDM, a larger Ω_M compared to CMB measurements from *Planck*. The discrepancy highlighted by Efstathiou (2024) is measured using a very limited subsample of the data included in the two compilations (< 20% of

[1] Following the dark energy equation of state parametrization $w(a) = w_0 + w_a(1 - a)$.

the data, corresponding to only bright events at high-z). Comp
the entire samples, however, the discrepancies are at the 0.01
level, at both high and low redshifts (Fig. 1).

In this paper, we do not address DESI results or discrepa
from *Planck*, and in the spirit of blind analyses we do not com
on the [dis]agreement with respect to a cosmological constant
response addresses the 0.04 mag discrepancy observed by Efsta
(2024) between the DES-SN5YR and Pantheon+ and we explai
reasons for this mismatch. We focus on the 118 low-z Found
events and 145 high-z DES events that overlap in Pantheon+
DES-SN5YR and consider the distance modulus offset:

$$\Delta\mu_{\rm offset} = \left\langle \mu_{\rm Pantheon+} - \mu_{\rm DES-SN5YR} \right\rangle_{\rm Foundation} - \left\langle \mu_{\rm Pantheon+} - \mu_{\rm DES-SN5YR} \right\rangle_{\rm DES}$$

where $\langle \mu_{\rm Pantheon+} - \mu_{\rm DES-SN5YR} \rangle$ is the mean differenc
tween Pantheon+ and DES-SN5YR distance moduli ($\mu_{\rm Pant}$
and $\mu_{\rm DES-SN5YR}$, respectively) computed from the inverse-var
weighted average over the overlapping Foundation or DES SNe. S
we only use SNe Ia to measure *relative* distances, any constant
between the two datasets would be absorbed by a combinati
the Hubble constant H_0 and SN Ia absolute magnitude M_0, and not
the cosmological parameters of interest here. In other words, if the
distance moduli from Pantheon+ and DES-SN5YR differed by the
same amount at both low and high redshifts, this would not affect the
inferred cosmology.

We note that Efstathiou (2024) did not use SN distance moduli μ,
but instead defined SN magnitudes as $m = \mu - M_0$, with M_0 fixed to
-19.33. Using this definition, Efstathiou (2024) found that,

$$\left\langle m_{\rm Pantheon+} - m_{\rm DES-SN5YR} \right\rangle_{\rm Foundation} \sim -0.05, \quad (2)$$

$$\left\langle m_{\rm Pantheon+} - m_{\rm DES-SN5YR} \right\rangle_{\rm DES} \sim -0.01, \quad (3)$$

suggesting that the most significant discrepancies between Pantheon+
and DES-SN5YR are in the analyses of the Foundation SN sample.
However, this approach implicitly assumes that M_0 is the same for
Pantheon+ and DES-SN5YR, which is not true because M_0 depends
on the light curve model training and analysis, which differ between
these two analyses. We therefore focus on the quantity $\Delta\mu_{\rm offset}$ (Eq. 1)
as it eliminates any confusion in the definition of M_0.

We provide a brief analysis recap in Sec. 3. The main reasons for
the observed discrepancy is given in Sections 4 and 5, and some
concluding remarks are in Sec. 6.

3 SNE IA STANDARDIZATION AND THE ROLE OF BIAS CORRECTIONS

Here, we briefly summarize the main steps necessary to standardize
SNe Ia brightnesses and correct for selection biases. The first step
to standardize SN brightnesses is to fit each SN light-curve for the
parameters $\{m_x, x_1, c\}$, which are the amplitude, stretch, and colour
of a SN, respectively (Guy et al. 2007; Betoule et al. 2014). For each
SN, these parameters are used to measure its standardized apparent
magnitude, m_x (Tripp 1998)

$$m_x^{\rm std} = m_x + \alpha x_1 - \beta c + \gamma G_{M_\star} \quad (4)$$

where α, β and γ are globally fitted nuisance parameters modelling
the stretch-, colour- and host- luminosity dependencies respectively.
$G_{M_\star}$ is a $\pm 1/2$ step function that describes the magnitude offset
observed between SNe found in high stellar mass ($M_\star > 10^{10} M_\odot$)
and low stellar mass ($M_\star < 10^{10} M_\odot$) galaxies (the so-called 'mass

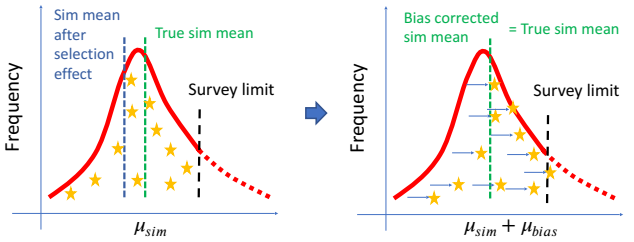

Figure 2. *Left panel*: Derived distances from simulated SN events $\mu_{\rm sim}$ for SNe in a given 4D bin of $z, x_1, c, M_\star$. The derived mean of the simulated data (blue vertical dashed line) is biased compared to the true simulated mean (green vertical dashed line). *Right panel*: Simulation-derived bias corrections ($\mu_{\rm bias}$) are added to *every* SN Ia in the bin (horizontal arrows) such that the derived mean aligns with the true mean. The correction depends on the SN Ia light curve model, scatter model, and instrumental noise.

step'). SN standardized apparent brightnesses are used to measure
SN distance moduli μ, defined as

$$\mu = m_x^{\rm std} - \mu_{\rm bias} - M_0 \quad (5)$$

where M_0 is the SN absolute brightness (fully degenerate with H_0).
The term $\mu_{\rm bias}$ corrects each SN distance for selection effects and
analysis biases. $\mu_{\rm bias}$ are determined from large simulations and are
defined as $\mu_{\rm bias} = \mu_{\rm sim} - \mu_{\rm true}$, where $\mu_{\rm sim} = m_x^{\rm std} - M_0$ are the
derived SN distances for simulated SN events and $\mu_{\rm true}$ are the true
simulated SN distances. We discuss $\mu_{\rm bias}$ in more detail below.

Most SN surveys are magnitude-limited. SNe Ia are intrinsically
variable objects, with bluer ($c < 0$) and longer duration ($x_1 > 0$)
explosions being brighter than redder ($c < 0$) and shorter duration
($x_1 < 0$) explosions. While the standardisation process (Eq. 4) re-
sults in nearly uniform brightness, the pre-standardized brightness
variation is more than 1 mag. This variation would not lead to a
bias in the magnitudes $m_x^{\rm std}$ in the hypothetical case that all SN Ia
have exactly the same brightness after standardisation, without error.
However, a $\sim$15% variation in brightness remains after standardiza-
tion, composed of remaining intrinsic variation in the explosions,
measurement noise, and modelling error. Detected SNe Ia have a se-
lection bias that preferentially includes intrinsically brighter events
near the magnitude limit of the survey (as defined by a selection
function). This selection effect results in a distance bias that $\mu_{\rm bias}$ in
Eq. 4 corrects for; without this bias correction, the cosmology results
would be significantly altered.

We illustrate this bias in Figure 2. The left panel represents the
$\mu_{\rm sim}$ distribution of simulated SNe Ia in a given 4-dimensional bin
of redshift, stretch, colour, and host stellar mass and only events
brighter than the detection limit are observed. The bias correction
($\mu_{\rm bias}$) adjusts all of the simulated SNe in the given bin such that the
derived mean of $\mu_{\rm sim}$ matches the true mean, $\mu_{\rm true}$, that would be
measured without selection bias.

In both the DES-SN5YR and Pantheon+ analyses, BBC models
selection biases using large simulations and interpolates $\mu_{\rm bias}$ in the
4-dimensional space mentioned above. In these large simulations, we
model the survey cadence, instrument characteristics, survey selec-
tion effects and the true distribution of SN Ia magnitudes. The latter
includes SN Ia populations of stretch and colour to define a mean
brightness model, as well as an "intrinsic scatter" model to account
for brightness variations about the mean model.

The intrinsic distribution of SN Ia magnitudes is described by a
physically-motivated model that captures features such as intrinsic
colour variation and host galaxy dust. This model is calibrated and

Table 1. Distance modulus offsets between Foundation (low-z) and DES (high-z) SNe common to DES-SN5YR and Pantheon+ compilations. The "Contribution to $\Delta\mu_{\rm offset}$" column shows the size of the change in $\Delta\mu_{\rm offset}$ due to each effect. The "Remaining $\mu_{\rm offset}$" column shows the offset remaining after that effect has been reverted or removed.

Analysis changes applied to DES-SN5YR	Contribution to $\Delta\mu_{\rm offset}$ [mag]	Remaining $\Delta\mu_{\rm offset}$ [mag]
None		**−0.042**
Revert to Pantheon+ intrinsic scatter model (∗)	**0.008**	**−0.034**
Revert to Pantheon+ host stellar mass estimations	**0.010**	**−0.024**
Remove offset due to different selection functions (‡)	**0.016**	**−0.008**

(∗) Pantheon+ used the original BS21 intrinsic scatter model. DES-SN5YR included this model in the systematic error budget, but used an improved version of the BS21 model for the nominal analysis.

(‡) This offset arises because the different DES subsamples have different corrections for selection functions. See Section 5.

fitted using data to reproduce the observed distributions and correlations of SN Ia parameters. As more data have been collected, the scatter model has continuously improved. The first attempt at a model beyond a coherent mag shift at all epochs and wavelengths was a simple spectral-energy-distribution (SED) intrinsic scatter model (Kessler et al. 2013, based on Guy et al. 2010 and Chotard et al. 2011), and it was used in the original Pantheon analysis (Scolnic et al. 2018) and DES-SN3YR (Brout et al. 2019b). Next, a significant update based on the properties of dust in SN host galaxies (Brout & Scolnic 2021) was used in Pantheon+. Finally, an updated version of the dust model (Popovic et al. 2023) was used in DES-SN5YR (see Section 4). The final bias correction applied to each SN Ia depends on the convolution of sample selection and the simulation of instrumental noise and intrinsic scatter.

4 MAJOR ANALYSIS IMPROVEMENTS BETWEEN Pantheon+ AND DES-SN5YR

The DES-SN5YR analysis introduced several improvements compared to the Pantheon+ analysis, in terms of the light-curve fitting model (upgrading from SALT2 to SALT3), intrinsic scatter model used in bias corrections, estimates of host galaxy stellar masses, and photometric calibration (using the latest DES internal calibration). A comprehensive list of these improvements is presented and discussed in Appendix A. In this section, we discuss the two analysis updates that have a significant impact on $\Delta\mu_{\rm offset}$ and summarize our results in Table 1.

(1) SN Ia Intrinsic scatter model: This model is essential to simulate and estimate accurate bias corrections on measured SN distances (Eq. 5 and Section 3). Both Pantheon+ and DES-SN5YR use a model for scatter in which the colour of SN Ia is a combination of intrinsic variation and reddening by host-galaxy dust, which itself depends on host galaxy properties (Brout & Scolnic 2021). This model is described by a set of 12 free parameters: 4 parameters characterizing intrinsic SN colour variations (mean and standard deviations of intrinsic colour and intrinsic β) + 8 parameters characterizing dust properties and their dependency on the host galaxy (mean and standard deviations of R_V and dust extinction exponential coefficient τ in high and low mass galaxies).

Pantheon+ used the dust parameters originally presented in Brout & Scolnic (2021), which were manually tuned such that the `SNANA` simulation reproduces the trends observed in data. In DES-SN5YR, we improved the measurement of these 12 parameters using the forward-modelling fitting method in Popovic et al. (2023). The differences between the colour/dust parameters used in Pantheon+ and DES-SN5YR are presented in Table 3 of Vincenzi et al. (2024).

Despite its overly simplistic approach to evaluating dust parameters, the original Pantheon+ modelling approach was still considered plausible, and therefore included in the DES-SN5YR analysis as a potential source of systematic uncertainty. In Figs. 13-15 and Table 8 in Vincenzi et al. (2024), we present the effects of this source of systematic (labelled as 'BS21') and show that using the BS21 intrinsic scatter model (instead of the nominal model from Popovic et al. 2023) introduces an offset of ∼0.010 mag between the low- and high-redshift samples of the DES-SN5YR Hubble diagram.

(2) Host masses: In DES-SN5YR, host-galaxy stellar masses have been updated for DES using deeper coadd photometry (Wiseman et al. 2020), and also updated for the low-z samples (Foundation, CfA and CSP) to ensure that the same galaxy SED fitting method was used for both the high-z and low-z samples (§ 2.5 in Vincenzi et al. 2024). For the Foundation subset of DES-SN5YR, the host masses of 10 SNe Ia (out of 118 total common between DES-SN5YRand Pantheon+) were changed from low-mass galaxies to high-mass galaxies ($> 10^{10} M_\odot$), and vice-versa 3 were changed from a high-mass to low-mass galaxy ($< 10^{10} M_\odot$). For the DES subset, the host masses of 10 (out of 145 common between DES-SN5YRand Pantheon+) were changed to low-mass galaxies, and 2 were changed to high-mass galaxies. Comparing the common SNe, the average difference in host stellar mass between Pantheon+ and DES-SN5YR is −0.16 dex for Foundation SN hosts and +0.07 dex for DES SN hosts. Neither analysis explicitly accounted for the host mass uncertainties, which results in a modest underestimate of systematics uncertainties.

Both analysis improvements contribute to the discrepancies highlighted by Efstathiou (2024). To quantify the impact that the analysis improvements in DES-SN5YR would have on Pantheon+, one would ideally re-analyze Pantheon+ sample using current codes and methods. However, such a re-analysis on a 3-year old sample is technically challenging on a short time-scale. Instead, it is sufficient to take the more practical approach of re-analyzing DES-SN5YR by substituting Pantheon+ modeling choices.

In Table 1, we show changes in $\Delta\mu_{\rm offset}$ when reverting the DES-SN5YR intrinsic scatter model and host mass values to match what was used in Pantheon+. The observed $\Delta\mu_{\rm offset}$ is reduced from −0.042 mag to −0.024 mag (43% reduction). The DES-SN5YR error budget adequately accounts for systematics related to the choice of intrinsic scatter model, but both Pantheon+ and DES-SN5YR underestimated uncertainties due to host stellar masses. We have estimated the missing systematic uncertainty related to host stellar mass: the total DES-SN5YR systematic error on w (assuming Flat$w$CDM) and w_0 or w_a (assuming Flatw_0w_aCDM) increase by less than 3%.

Finally, we estimate how DES-SN5YR cosmological results would change when reverting to the older (less accurate) scatter model

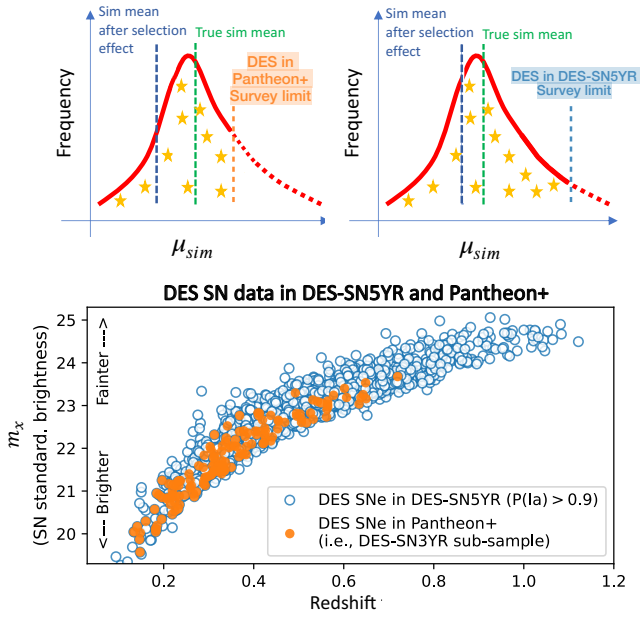

Figure 3. Illustration of the different selection functions characterizing the DES sub-samples in DES-SN5YR and Pantheon+. The *upper-left* panel illustrates the DES SNe included in Pantheon+ which are intentionally selected to be the brightest and highest signal-to-noise DES SNe, whereas the *upper-right* panel shows DES-SN5YR with a significantly more complete sample. In the lower panel, we show SALT3-fitted m_x *vs* redshift for the real DES data in DES-SN5YR (empty blue circles) and in Pantheon+ (filled orange circles). For DES-SN5YR, we only plot SNe with high ($> 90\%$) probability of being type Ia. Even at lower redshifts ($z < 0.4$), the sample of DES SNe in Pantheon+ is not complete and clearly biased toward the brightest events.

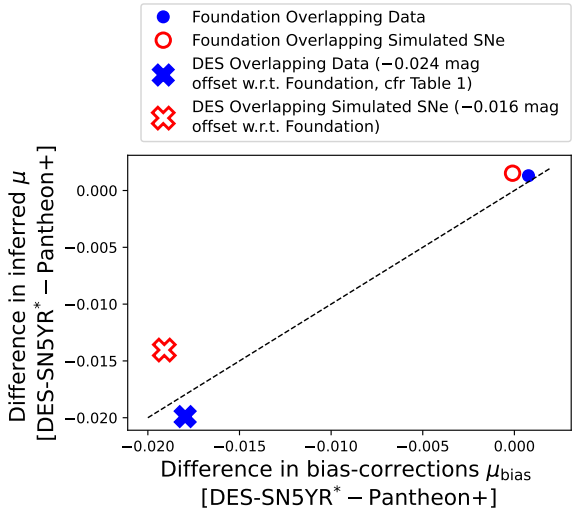

Figure 4. For the DES and Foundation sub-samples of overlapping SNe between DES-SN5YR* and Pantheon+, we compare the difference in bias corrections μ_{bias} with the difference in distance moduli, μ. Differences relative to the Foundation (DES) sub-sample of overlapping data are marked with circles (crosses). Filled blue symbols correspond to differences in the real data, while empty red symbols correspond to differences estimated from simulations. Instead of using the original DES-SN5YR distance moduli, we use distances from a re-analysis using the Pantheon+ modelling as described in Section 4. For this reason, differences in measured distance moduli from the data are -0.024 (and not -0.042, see Table 1). To avoid confusion with different M_0, we subtract 0.04 mag from all the DES-SN5YR bias-corrections. Using simulations, we quantify the expected differences in μ between the DES sub-samples in Pantheon+ and DES-SN5YR to be -0.016.

and host properties from Pantheon+. The DES-SN5YR evidence for evolving dark energy is mildly reduced from 3.9σ to 3.3σ.

4.1 A note on bias-corrected distances in Pantheon+ and DES-SN5YR

The updated light curve and intrinsic scatter models resulted in a constant shift of 0.04 mag between bias-corrections in Pantheon+ and DES-SN5YR. While this 0.04 mag offset may confuse the interpretation of distances in the two analyses, this offset *has no effect on the cosmological results of DES-SN5YR or Pantheon+* because SN dark energy constraints are insensitive to global offsets in the distances.

5 MODELLING SELECTION EFFECTS

In Section 4, we show the impact of explicit analysis changes between Pantheon+ and DES-SN5YR. However, even if both analyses were identical in their methods and assumptions, we still expect to see a non-zero $\Delta\mu_{\rm offset}$ when performing a direct object-to-object comparison between the Pantheon+ and DES-SN5YR data compilations. The reason for this expectation is that the selection of the overlapping DES sub-sample embedded in Pantheon+ and DES-SN5YR is very different. As noted in the previous two Sections, changes to the selection function also change the bias corrections.

The effects of bias corrections on Pantheon+ and DES-SN5YR are illustrated in Fig. 3. The Pantheon+ analysis included the DES-SN3YR sub-sample, i.e., a sample of the *brightest* DES SNe for which spectroscopic follow-up of the live transient was available (207 SNe). Therefore, this sample is characterized by *strong selection biases* and requires *large bias corrections*. In sharp contrast to this earlier analysis, the DES-SN5YR analysis used photometric classification (Möller & de Boissière 2020; Qu et al. 2021; Möller et al. 2022) and selected all DES SNe for which the host spectroscopic redshifts was available. This sub-sample is significantly deeper in redshift and more complete, and it includes a significantly larger number of SNe (1635 SNe).

These fundamental differences in selection functions result in different bias corrections between the Pantheon+ and DES-SN5YR analyses and make it difficult to compare the overlapping events as proposed in Efstathiou (2024). Since we can accurately model the selection functions of the DES subsample included in Pantheon+ and the DES-SN5YR sample, we can reproduce this effect using simulations. We generate a large ($\times$10) DES-like simulation and apply the Pantheon+ DES selection function and the DES-SN5YR selection function to obtain two samples that reflect the DES subsamples included in Pantheon+ and DES-SN5YR. We identify the overlapping simulated events between the two samples and compare their bias-corrections.

In Fig. 4, we compare differences in bias corrections, $\mu_{\rm bias}$(DES-SN5YR*) $-$ $\mu_{\rm bias}$(Pantheon+) with differences in distance moduli μ(DES-SN5YR*) $-$ μ(Pantheon+). For this comparison, DES-SN5YR* is analyzed using Pantheon+ modelling choices as described in Section 4 and Table 1. Using a consistent analysis avoids conflating multiple effects and more clearly shows the effect of bias corrections described in this section. As shown in Fig. 4,

for the low-z samples ($z < 0.1$), the difference in $\mu_{\rm bias}$ is negligible because the sample selection is nearly the same for the two analyses. At higher redshifts ($z > 0.1$), the data show large differences in $\mu_{\rm bias}$ (~ 0.02) that are directly reflected into differences in μ. These differences are reproduced by our simulations at the 5 millimag level. Our simulations show that differences in $\mu_{\rm bias}$ are expected when analysing the two subsamples in the context of the (more biased towards brighter events) Pantheon+ analysis or in the context of the (significantly more complete) DES-SN5YR analysis. In particular, both in data and simulations we find that Pantheon+ bias corrections differ by approximately ~ -0.02 mag.

From our simulations, we estimate that this bias-correction effect contributes ~0.016 mag to the $\Delta\mu_{\rm offset}$ observed by Efstathiou (2024). However, we highlight that this effect is only important when performing an object-to-object comparison like the one presented by Efstathiou (2024). This effect is not relevant for the *full-sample* Hubble diagram comparison shown in Fig. 1 because each full sample is corrected for their specific sample biases. In other words, in Fig. 1 we compare the bias-corrected 'Data mean' at each redshift bin (following the terminology of Fig. 2) rather than individual objects removed from their original context.

6 CONCLUSION

Efstathiou (2024) noted a 0.04 mag low-vs-high redshift distance offset (Eq. 1) between overlapping Pantheon+ and DES-SN5YR events. We have investigated this offset and find that it is explained as follow.

- **Two analysis improvements since Pantheon+**: These improvements are related to the intrinsic scatter model and host stellar mass estimates, and account for 0.018 mag discrepancy between Pantheon+ and DES-SN5YR (from −0.042 to −0.024, see Table 1);
- **Selection differences between Pantheon+ and DES-SN5YR:** Larger distance bias corrections are required for the more heavily biased Pantheon+ sample of spectroscopically identified events, compared to smaller bias corrections for the more complete sample of photometrically classified events in DES-SN5YR (Fig. 4). This difference in selection functions does not affect cosmology results, but leads to misleading conclusions in an object-to-object comparison like the one presented by Efstathiou (2024), where only 20% of the brightest SNe are selected from both analyses. This effect account for an additional 0.016 mag discrepancy between Pantheon+ and DES-SN5YR (from −0.024 to −0.008, see Table 1). This biased comparison can be avoided by comparing the binned Pantheon+ and DES-SN5YR Hubble diagrams as shown in Fig. 1.

Near the completion of our response to Efstathiou (2024), Notari et al. (2024) performed a re-analysis of Pantheon+ and DES-SN5YR in which common SNe are excluded from one sample in order to perform a combined analysis of the two independent samples. We have not performed a detailed investigation of their analysis or claims, but we note a few qualitative issues with their analysis. First, removing or adding events changes the selection criteria and hence requires updated bias corrections. Second, while the 0.04 mag M_0 offset between Pantheon+ and DES-SN5YR distances does not impact cosmology results from each separate analysis, this offset can bias results from combining distances without a re-analysis using consistent SN Ia modelling and bias corrections.

In conclusion, we hope that this post-publication investigation offers the community valuable insights into the DES-SN5YR and Pantheon+ analyses, and it reinforces one of the main conclusions drawn from the DES-SN5YR analysis (Vincenzi et al. 2024): the limiting factor and largest source of systematics in current SN Ia cosmology analysis is the modelling of intrinsic scatter and SN-host correlations in bias corrections. Nevertheless, these uncertainties are usually included in the error budget of the current data sets, and thus accounted for in the uncertainties on cosmological parameters. In particular, the DES-SN5YR analysis accounted for several additional sources of systematic uncertainties related to intrinsic scatter and SN-host correlations that have not been included in any previous analysis (including Pantheon+). Here we identified one untracked systematic uncertainty due to host galaxy measurement uncertainties, which increases the previously reported uncertainties by about 3%.

Upcoming data from the Zwicky Transient Factory (Rigault et al. 2024), the Vera C. Rubin Observatory, and the Roman Space Telescope will improve our understanding and control of these sources of systematics.

CONTRIBUTION STATEMENT AND ACKNOWLEDGMENTS

M.V. led the primary analysis and drafted the manuscript; R.K. and P.S. contributed substantially to the analysis, manuscript preparation, and figure curation. J.L. contributed to the analysis and provided comments on the manuscript. D.S. and T.M.D. advised on the analysis, provided detailed feedback on the manuscript, and served as internal reviewers. A.M., B.R., B.P., C.L., D.B., M. Sa., M.Sm., M.Su., P.W., L.G., R.C. and J.Mu. provided comments on the manuscript. The remaining authors have made contributions to this paper that include, but are not limited to, the construction of DECam and other aspects of collecting the data; data processing and calibration; developing broadly used methods, codes, and simulations; running the pipelines and validation tests; and promoting the science analysis. This paper has gone through internal review by the DES collaboration.

Funding for the DES Projects has been provided by the U.S. Department of Energy, the U.S. National Science Foundation, the Ministry of Science and Education of Spain, the Science and Technology Facilities Council of the United Kingdom, the Higher Education Funding Council for England, the National Center for Supercomputing Applications at the University of Illinois at Urbana-Champaign, the Kavli Institute of Cosmological Physics at the University of Chicago, the Center for Cosmology and Astro-Particle Physics at the Ohio State University, the Mitchell Institute for Fundamental Physics and Astronomy at Texas A&M University, Financiadora de Estudos e Projetos, Fundação Carlos Chagas Filho de Amparo à Pesquisa do Estado do Rio de Janeiro, Conselho Nacional de Desenvolvimento Científico e Tecnológico and the Ministério da Ciência, Tecnologia e Inovação, the Deutsche Forschungsgemeinschaft and the Collaborating Institutions in the Dark Energy Survey.

The Collaborating Institutions are Argonne National Laboratory, the University of California at Santa Cruz, the University of Cambridge, Centro de Investigaciones Energéticas, Medioambientales y Tecnológicas-Madrid, the University of Chicago, University College London, the DES-Brazil Consortium, the University of Edinburgh, the Eidgenössische Technische Hochschule (ETH) Zürich, Fermi National Accelerator Laboratory, the University of Illinois at Urbana-Champaign, the Institut de Ciències de l'Espai (IEEC/CSIC), the Institut de Física d'Altes Energies, Lawrence Berkeley National Laboratory, the Ludwig-Maximilians Universität München and the associated Excellence Cluster Universe, the University of Michigan, NSF's NOIRLab, the University of Nottingham, The Ohio State University, the University of Pennsylvania, the University of Portsmouth, SLAC National Accelerator Laboratory, Stanford University, the Uni-

versity of Sussex, Texas A&M University, and the OzDES Membership Consortium.

R.K. is supported by DOE grant DE-SC0009924. T.M.D. is the recipient of an Australian Research Council Laureate Fellowship (FL180100168) funded by the Australian Government. A.M. is supported by the ARC Discovery Early Career Researcher Award (DECRA) project number DE230100055. L.G. acknowledges financial support from AGAUR, CSIC, MCIN and AEI 10.13039/501100011033 under projects PID2023-151307NB-I00, PIE 20215AT016, CEX2020-001058-M, ILINK23001, COOPB2304, and 2021-SGR-01270. We acknowledge the University of Chicago's Research Computing Center for their support of this work.

Based in part on observations at Cerro Tololo Inter-American Observatory at NSF's NOIRLab (NOIRLab Prop. ID 2012B-0001; PI: J. Frieman), which is managed by the Association of Universities for Research in Astronomy (AURA) under a cooperative agreement with the National Science Foundation. Based in part on data acquired at the Anglo-Australian Telescope. We acknowledge the traditional custodians of the land on which the AAT stands, the Gamilaraay people, and pay our respects to elders past and present.

The DES data management system is supported by the National Science Foundation under Grant Numbers AST-1138766 and AST-1536171. The DES participants from Spanish institutions are partially supported by MICINN under grants ESP2017-89838, PGC2018-094773, PGC2018-102021, SEV-2016-0588, SEV-2016-0597, and MDM-2015-0509, some of which include ERDF funds from the European Union. IFAE is partially funded by the CERCA program of the Generalitat de Catalunya. Research leading to these results has received funding from the European Research Council under the European Union's Seventh Framework Program (FP7/2007-2013) including ERC grant agreements 240672, 291329, and 306478. We acknowledge support from the Brazilian Instituto Nacional de Ciência e Tecnologia (INCT) do e-Universo (CNPq grant 465376/2014-2). This manuscript has been authored by Fermi Research Alliance, LLC under Contract No. DE-AC02-07CH11359 with the U.S. Department of Energy, Office of Science, Office of High Energy Physics.

DATA AVAILABILITY

All data used in this analysis are publicly available at `https://github.com/PantheonPlusSH0ES/DataRelease` and `https://github.com/des-science/DES-SN5YR`.

REFERENCES

Abbott T. M. C., et al., 2019, ApJ, 872, L30
Betoule M., et al., 2014, A&A, 568, A22
Brout D., Scolnic D., 2021, ApJ, 909, 26
Brout D., et al., 2019a, ApJ, 874, 106
Brout D., et al., 2019b, ApJ, 874, 150
Brout D., et al., 2022a, ApJ, 938, 110
Brout D., et al., 2022b, ApJ, 938, 111
Burke D. L., et al., 2018, AJ, 155, 41
Carron J., Mirmelstein M., Lewis A., 2022, J. Cosmology Astropart. Phys., 2022, 039
Chotard N., et al., 2011, A&A, 529, L4
DES Collaboration et al., 2024, arXiv e-prints, p. arXiv:2401.02929
DESI Collaboration et al., 2024, arXiv e-prints, p. arXiv:2404.03002
Efstathiou G., 2024, arXiv e-prints, p. arXiv:2408.07175
Foley R. J., et al., 2017, Monthly Notices of the Royal Astronomical Society, 475, 193
Guy J., et al., 2007, A&A, 466, 11
Guy J., et al., 2010, A&A, 523, A7
Hicken M., et al., 2009, ApJ, 700, 331
Hicken M., et al., 2012, ApJS, 200, 12
Hinton S., Brout D., 2020, The Journal of Open Source Software, 5, 2122
Kenworthy W. D., et al., 2021, ApJ, 923, 265
Kessler R., Scolnic D., 2017, ApJ, 836, 56
Kessler R., et al., 2009, PASP, 121, 1028
Kessler R., et al., 2013, ApJ, 764, 48
Krisciunas K., et al., 2017, AJ, 154, 211
Möller A., de Boissière T., 2020, MNRAS, 491, 4277
Möller A., et al., 2022, MNRAS, 514, 5159
Notari A., Redi M., Tesi A., 2024, arXiv e-prints, p. arXiv:2411.11685
Planck Collaboration et al., 2020a, A&A, 641, A1
Planck Collaboration et al., 2020b, A&A, 641, A6
Popovic B., Brout D., Kessler R., Scolnic D., 2023, ApJ, 945, 84
Qu H., Sako M., Möller A., Doux C., 2021, AJ, 162, 67
Rigault M., et al., 2024, arXiv e-prints, p. arXiv:2409.04346
Rubin D., et al., 2015, ApJ, 813, 137
Rubin D., et al., 2023, arXiv e-prints, p. arXiv:2311.12098
Sánchez B. O., et al., 2024, arXiv e-prints, p. arXiv:2406.05046
Scolnic D. M., et al., 2018, ApJ, 859, 101
Scolnic D., et al., 2022, ApJ, 938, 113
Sevilla-Noarbe I., et al., 2021, The Astrophysical Journal Supplement Series, 254, 24
Taylor G., et al., 2023, MNRAS, 520, 5209
Tripp R., 1998, A&A, 331, 815
Vincenzi M., et al., 2024, arXiv e-prints, p. arXiv:2401.02945
Wiseman P., et al., 2020, MNRAS, 495, 4040
Zuntz J., et al., 2015, Astronomy and Computing, 12, 45

APPENDIX: ADDITIONAL ANALYSIS IMPROVEMENTS IN DES-SN5YR FROM Pantheon+

In this Appendix, we list the additional analysis changes introduced in DES-SN5YR compared to Pantheon+. In contrast to the analysis updates discussed in Section 4, the updates discussed here have a negligible effect on the $\Delta\mu_{\rm offset}$ discussed by Efstathiou (2024).

Light-curve fitting model: Pantheon+ used the SALT2 light-curve model from Betoule et al. (2014) to fit each event for the standardizaton parameters $\{m_x, x_1, c\}$. In DES-SN5YR, we upgraded to the recently published SALT3 model (Kenworthy et al. 2021), after carefully testing the SALT2 and SALT3 models on published cosmological samples (Taylor et al. 2023).

We compare the SALT2 and SALT3 standardized $m_x^{\rm std}$ in Fig. 1a and find that differences are negligible. Therefore, we do not expect the differences between SALT2 and SALT3 models to explain any of the trends highlighted by Efstathiou (2024).

While the $m_x^{\rm std}$ differences are small, its uncertainty is significantly reduced in DES-SN5YR (see Fig. 1b). This reduction is due to the broader wavelength range covered by the SALT3 model. The SALT3 mean rest-frame wavelength per band extends 1000 Å farther into the near-infrared compared to SALT2 (from 7000 Å to 8000 Å), enabling the use of Foundation and DES z-band data at low redshifts (where observed z-band correspond to ∼8000 Å in the rest-frame). The SALT3 model therefore results in larger weight given to low-z SNe in DES-SN5YR compared to Pantheon+.

Calibration: Photometric calibration for both Pantheon+ and DES-SN5YR is presented by (Brout et al. 2022b) using a cross-calibration approach. For the Foundation SN sample, the same calibration was used for both Pantheon+ and DES-SN5YR. However, the DES subsets in Pantheon+and DES-SN5YR are treated independently

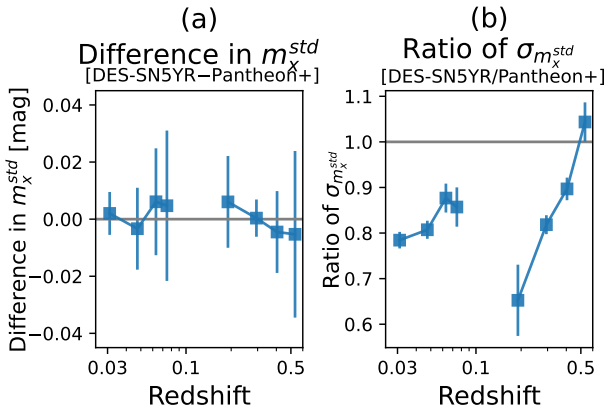

Figure 1. *Left panel*: Median $m_x^{\rm std}$ difference vs. redshift (and error on the median) for common SNe in DES-SN5YR and Pantheon+. Across all redshifts, differences in $m_x^{\rm std}$ are consistent with zero. *Right panel*: ratio of $m_x^{\rm std}$ uncertainties between DES-SN5YR and Pantheon+. For a more direct comparison, we measure $m_x^{\rm std}$ and its uncertainty using the same nuisance parameters for both DES-SN5YR and Pantheon+: $\alpha = 0.15$, $\beta = 3.1$, $\gamma = 0$.

because each sample was reprocessed independently. The same Scene Modelling Photometry code (Brout et al. 2019a; Sánchez et al. 2024) was used to produce light curves for both sub-samples, but the DES survey calibration was updated towards the end of the survey (compare Burke et al. 2018; Sevilla-Noarbe et al. 2021) and therefore DES-SN5YR required slightly different AB calibration offsets (−0.004 to 0.009 mag) compared to the earlier DES-SN3YR data release included in Pantheon+. The final AB calibration offsets used in Pantheon+ and DES-SN5YR are presented in Table 3 of Brout et al. (2022b) and their uncertainties propagated in our systematic error budget. These calibration offsets are significantly smaller than the observed $\Delta\mu_{\rm offset}$ (Eq. 1) and are therefore unlikely to have much impact on it.

Nuisance parameters: Pantheon+ and DES-SN5YR each used their BBC-fitted nuisance parameters for SN standardization and distance estimates: Pantheon+ found α=0.148, β=3.09 and γ=0, while DES-SN5YR found α=0.161, β=3.12 and γ=0.038. Therefore, when comparing distances for the same events across the two analyses, differences are expected.

Beams with Bias Corrections: the BBC framework was used both in Pantheon+ and DES-SN5YR, and there have been several code updates[2] between the publication of Pantheon+ and DES-SN5YR. One of the most significant code updates was related to the treatment of the parameter β in the calculation of the bias-corrections. In Pantheon+, the (wrong) *intrinsic* β parameter ($\beta_{\rm intr}$~2) was used in Eq. 4 to estimate bias corrections, instead of the effective β ($\beta_{\rm eff}$~3), which is a combination of intrinsic β and extrinsic dust law.

We do not test this by reverting the entire DES-SN5YR to use the same SALT2 model as Pantheon+ because Fig. 1 shows that discrepancies are negligible. We also do not recompute the DES-SN5YR calibration because differences between calibration offsets applied to the DES sub-samples in Pantheon+ and DES-SN5YR are also significantly smaller than $\Delta\mu_{\rm offset}$.

[2] https://github.com/RickKessler/SNANA/blob/master/src/SALT2mu.c

Reprocessing DES-SN5YR using the (obsolete) Pantheon+ version of the BBC code does not have a significant effect on $\Delta\mu_{\rm offset}$. However, reprocessing the full Pantheon+ sample (not just the overlapping sample) using the current BBC code results in an average distance change of ~+0.005 mag at low-z ($z < 0.1$) and ~−0.005 mag at high-z ($z > 0.1$). Therefore, BBC code updates impact the overall Pantheon+ Hubble diagram. As a final test, we reprocessed the DES-SN5YR analysis (which was frozen nearly 1.5 years ago) with the current BBC code and found a distance change of ~0.001 mag between low-z and high-z.

AFFILIATIONS

[1] Department of Physics, University of Oxford, Denys Wilkinson Building, Keble Road, Oxford OX1 3RH, United Kingdom
[2] Department of Astronomy and Astrophysics, University of Chicago, Chicago, IL 60637, USA
[3] Kavli Institute for Cosmological Physics, University of Chicago, Chicago, IL 60637, USA
[4] Department of Physics & Astronomy, University College London, Gower Street, London, WC1E 6BT, UK
[5] Department of Physics and Astronomy, University of Pennsylvania, Philadelphia, PA 19104, USA
[6] School of Mathematics and Physics, University of Queensland, Brisbane, QLD 4072, Australia
[7] Department of Physics, Duke University Durham, NC 27708, USA
[8] Boston University Department of Astronomy, 725 Commonwealth Ave, Boston USA
[9] Institute of Space Sciences (ICE, CSIC), Campus UAB, Carrer de Can Magrans, s/n, 08193 Barcelona, Spain
[10] Institut d'Estudis Espacials de Catalunya (IEEC), 08034 Barcelona, Spain
[11] Centre for Gravitational Astrophysics, College of Science, The Australian National University, ACT 2601, Australia
[12] The Research School of Astronomy and Astrophysics, Australian National University, ACT 2601, Australia
[13] Centre for Astrophysics & Supercomputing, Swinburne University of Technology, Victoria 3122, Australia
[14] Univ Lyon, Univ Claude Bernard Lyon 1, CNRS, IP2I Lyon / IN2P3, IMR 5822, F-69622, Villeurbanne, France
[15] Department of Physics and Astronomy, Baylor University, Waco, TX 76706, USA
[16] Aix Marseille Univ, CNRS/IN2P3, CPPM, Marseille, France
[17] Physics Department, Lancaster University, Lancaster, LA1 4YB, UK
[18] School of Physics and Astronomy, University of Southampton, Southampton, SO17 1BJ, UK
[19] Cerro Tololo Inter-American Observatory, NSF's National Optical-Infrared Astronomy Research Laboratory, Casilla 603, La Serena, Chile
[20] Laboratório Interinstitucional de e-Astronomia - LIneA, Rua Gal. José Cristino 77, Rio de Janeiro, RJ - 20921-400, Brazil
[21] Fermi National Accelerator Laboratory, P. O. Box 500, Batavia, IL 60510, USA
[22] Physik-Institut, University of Zurich, Winterthurerstrasse 190, CH-8057 Zurich, Switzerland
[23] University Observatory, Faculty of Physics, Ludwig-Maximilians-Universität, Scheinerstr. 1, 81679 Munich, Germany
[24] Instituto de Astrofisica de Canarias, E-38205 La Laguna, Tenerife, Spain
[25] Universidad de La Laguna, Dpto. Astrofísica, E-38206 La Laguna, Tenerife, Spain
[26] Institut de Física d'Altes Energies (IFAE), The Barcelona Institute of Science and Technology, Campus UAB, 08193 Bellaterra (Barcelona) Spain
[27] Hamburger Sternwarte, Universität Hamburg, Gojenbergsweg 112, 21029 Hamburg, Germany
[28] California Institute of Technology, 1200 East California Blvd, MC 249-17, Pasadena, CA 91125, USA
[29] Instituto de Fisica Teorica UAM/CSIC, Universidad Autonoma de Madrid, 28049 Madrid, Spain
[30] Institute of Cosmology and Gravitation, University of Portsmouth, Portsmouth, PO1 3FX, UK
[31] Center for Astrophysical Surveys, National Center for Supercomputing Applications, 1205 West Clark St., Urbana, IL 61801, USA
[32] Department of Astronomy, University of Illinois at Urbana-Champaign, 1002 W. Green Street, Urbana, IL 61801, USA
[33] Santa Cruz Institute for Particle Physics, Santa Cruz, CA 95064, USA
[34] Center for Cosmology and Astro-Particle Physics, The Ohio State University, Columbus, OH 43210, USA
[35] Department of Physics, The Ohio State University, Columbus, OH 43210, USA
[36] Center for Astrophysics | Harvard & Smithsonian, 60 Garden Street, Cambridge, MA 02138, USA
[37] Australian Astronomical Optics, Macquarie University, North Ryde, NSW 2113, Australia
[38] Lowell Observatory, 1400 Mars Hill Rd, Flagstaff, AZ 86001, USA
[39] Jet Propulsion Laboratory, California Institute of Technology, 4800 Oak Grove Dr., Pasadena, CA 91109, USA
[40] George P. and Cynthia Woods Mitchell Institute for Fundamental Physics and Astronomy, and Department of Physics and Astronomy, Texas A&M University, College Station, TX 77843, USA
[41] LPSC Grenoble - 53, Avenue des Martyrs 38026 Grenoble, France
[42] Institució Catalana de Recerca i Estudis Avançats, E-08010 Barcelona, Spain
[43] Perimeter Institute for Theoretical Physics, 31 Caroline St. North, Waterloo, ON N2L 2Y5, Canada
[44] Department of Astrophysical Sciences, Princeton University, Peyton Hall, Princeton, NJ 08544, USA
[45] Department of Physics, Carnegie Mellon University, Pittsburgh, Pennsylvania 15312, USA
[46] Kavli Institute for Particle Astrophysics & Cosmology, P. O. Box 2450, Stanford University, Stanford, CA 94305, USA
[47] SLAC National Accelerator Laboratory, Menlo Park, CA 94025, USA
[48] Centro de Investigaciones Energéticas, Medioambientales y Tecnológicas (CIEMAT), Madrid, Spain
[49] Ruhr University Bochum, Faculty of Physics and Astronomy, Astronomical Institute, German Centre for Cosmological Lensing, 44780 Bochum, Germany
[50] Department of Physics, Northeastern University, Boston, MA 02115, USA
[51] Computer Science and Mathematics Division, Oak Ridge National Laboratory, Oak Ridge, TN 37831
[52] Department of Physics, University of Michigan, Ann Arbor, MI 48109, USA
[53] Department of Astronomy, University of California, Berkeley, 501 Campbell Hall, Berkeley, CA 94720, USA
[54] Lawrence Berkeley National Laboratory, 1 Cyclotron Road, Berkeley, CA 94720, USA
[55] Max Planck Institute for Extraterrestrial Physics, Giessenbachstrasse, 85748 Garching, Germany
[56] Universitäts-Sternwarte, Fakultät für Physik, Ludwig-Maximilians Universität München, Scheinerstr. 1, 81679 München, Germany

This paper has been typeset from a TEX/LATEX file prepared by the author.